



DIGITAL ACCESS TO
SCHOLARSHIP AT HARVARD
DASH.HARVARD.EDU



HARVARD LIBRARY
Office for Scholarly Communication

Phenomenology of a top quark seesaw model

The Harvard community has made this article openly available. [Please share](#) how this access benefits you. Your story matters

Citation	Collins, Hael, Aaron Grant, and Howard Georgi. 2000. "Phenomenology of a Top Quark Seesaw Model." Phys. Rev. D 61 (5) (January 19). doi:10.1103/physrevd.61.055002.
Published Version	doi:10.1103/PhysRevD.61.055002
Citable link	http://nrs.harvard.edu/urn-3:HUL.InstRepos:28265576
Terms of Use	This article was downloaded from Harvard University's DASH repository, and is made available under the terms and conditions applicable to Other Posted Material, as set forth at http://nrs.harvard.edu/urn-3:HUL.InstRepos:dash.current.terms-of-use#LAA

The Phenomenology of a Top Quark Seesaw Model

Hael Collins[†], Aaron Grant[‡] and Howard Georgi^{*}

Harvard University

Cambridge, MA 02138, USA

[†]hael@feynman.harvard.edu

[‡]grant@feynman.harvard.edu

^{*}georgi@physics.harvard.edu

ABSTRACT

The top quark seesaw mechanism offers a method for constructing a composite Higgs field without the usual difficulties that accompany traditional technicolor or topcolor theories. The focus of this article is to study the phenomenology of the new physics required by this mechanism. After establishing a set of criteria for a plausible top quark seesaw theory, we develop two models, the first of which has a heavy weak singlet fermion with hypercharge $\frac{4}{3}$ while the second has, in addition, a heavy weak singlet hypercharge $-\frac{2}{3}$ fermion. At low energies, these theories contain one or two Higgs doublets respectively. We then derive the low energy effective Higgs potential in detail for the two-doublet theory as well as study the likely experimental signatures for both theories. A strong constraint on the one-doublet model is the measured value of the ρ parameter which permits the new heavy fermion to have a mass of about 5–7 TeV, when the Higgs has a mass greater than 300 GeV. In the two-doublet model, mixing of the new heavy $Y = -\frac{2}{3}$ fermion and the b quark affects the prediction for R_b . In order to agree with the current limits on R_b , the mass of this fermion should be at least 12 TeV. The mass of the heavy $Y = \frac{4}{3}$ fermion in the two-doublet model is not as sharply constrained by experiments and can be as light as 2.5 TeV.

August, 1999

1. Introduction

In recent years the standard model has been subjected to extraordinarily precise experimental tests [1]. All the evidence to date suggests that the usual picture of fundamental interactions, based on a spontaneously broken $SU(2) \times U(1)$ gauge symmetry, is quantitatively correct. However, the character of the symmetry breaking sector of the theory is still largely mysterious. Constraints derived from precision electroweak data suggest that the Higgs boson may be light [1], although this conclusion has been criticized on various grounds [2]. In addition, it has been argued [3] that models of electroweak symmetry breaking that involve large numbers of new strongly interacting $SU(2)$ doublet fermions are excluded by experiment. These constraints pose a significant challenge to traditional technicolor models [4] since such models typically predict a heavy Higgs boson, and often involve large numbers of new $SU(2)$ doublets.

These considerations suggest that the simplest technicolor mechanisms may not be realized in nature. An alternative scenario has been suggested [5], in which the composite Higgs field is “made” of ordinary standard model quarks. Indeed, the composite field $\bar{Q}_R \psi_L^3$, where ψ_L^3 is the (t, b) doublet and Q is a quark with electric charge $+2/3$, has the correct quantum numbers to play the role of the standard model Higgs boson. In models of this type, four-fermi operators that result from integrating out physics at a high scales bind the composite Higgs and break $SU(2)$ through the formation of a $\bar{Q}_R \psi_L^3$ condensate. The simplest models, in which $Q_R \equiv t_R$, predict a top mass that is too large. So it has been suggested that Q_R is simply a new isosinglet quark with the quantum numbers of t_R , and that the physical top quark mass comes about via a “see-saw” mechanism involving t and Q [6].

A full description of the top-condensate see-saw mechanism must involve new interactions at high scales. In particular, the four-fermi operators needed to bind the composite Higgs and break $SU(2)$ may come about as the result of integrating out the massive gauge bosons of a spontaneously broken “topcolor” gauge interaction [7]. So, in a sense, top-condensate models defer the problem of gauge symmetry breaking to a new $SU(2)$ singlet sector of the theory, whose interactions break topcolor.

In the present article, we discuss some of the issues involved in constructing topcolor models that are “complete,” in the sense that all gauge symmetry breaking is accomplished dynamically, without recourse to *ad hoc* phenomenological Higgs multiplets. In Sec. 2, we review the basic features of top condensate see-saw models. In Sec. 3, we discuss models

of physics above the scale of topcolor breaking, and delineate two classes of models that appear to be viable. In Sec. 4 we discuss the spectrum of composite Higgs bosons in these models. In Sec. 5, we study the phenomenology of these models at low energies, and present experimental constraints on the masses of new particles predicted by our models. Finally, Sec. 6 concludes.

2. The Development of the Top Quark Seesaw Mechanism.

As experiments placed larger and larger bounds on the mass of the top quark, it became tempting to speculate that the top quark plays a principal role in the breaking of electroweak symmetry. This observation led Nambu and others [8] to suggest that if some new interactions produced a top quark condensate, $\langle \bar{t}t \rangle$, this condensate would have the correct gauge properties to break $SU(2)_W \times U(1)_Y \rightarrow U(1)_{\text{em}}$. The interaction that he studied was the four-fermion interaction,

$$\mathcal{L} = \mathcal{L}_{\text{kinetic}} + G(\bar{\psi}_L t_R)(\bar{t}_R \psi_L^a). \quad (2.1)$$

Here, ψ_L is the usual left-handed third generation quark doublet and t_R is the right-handed top quark. Bardeen, Hill and Lindner [5], following Nambu, examined this interaction further by performing a renormalization group analysis of the low energy theory. By summing the graphs contributing to the W -propagator in the bubble approximation, they estimated that the scale associated with electroweak symmetry breaking, $v = 246 \text{ GeV}$, and the top quark mass are related by the Pagels-Stokar formula [9]

$$v^2 \approx \frac{N_c}{8\pi^2} m_t^2 \ln \frac{\Lambda^2}{m_t^2}. \quad (2.2)$$

For Λ of order 1 TeV, this indicates a top mass of order 600 GeV. The prediction of m_t can be lowered by taking the cutoff Λ to be very large. However, even for $\Lambda \sim M_{\text{Planck}}$, the predicted top quark mass is too large. Indeed, the detailed analysis of [5] indicates that $m_t = 218 \text{ GeV}$ for this value of Λ .

Apart from the top mass prediction, this theory for top condensation has several unappealing features. The interaction in (2.1) is not renormalizable and must be the low energy remnant of some new physics. More seriously, the strength of the interaction must be very precisely tuned in order to obtain $M_{W,Z} \ll \Lambda$. This is the usual gauge hierarchy problem.

The first difficulty was resolved when Hill [7] noticed that, through a Fierz rearrangement, the four-fermi interaction could be rewritten in a suggestive form. Indeed, we can make the substitution

$$(\bar{\psi}_{La}t_R)(\bar{t}_R\psi_L^a) \rightarrow -(\bar{\psi}_{La}\gamma_\mu\frac{1}{2}\lambda^A\psi_L^a)(\bar{t}_R\gamma^\mu\frac{1}{2}\lambda^At_R) + \mathcal{O}(N_c^{-1}). \quad (2.3)$$

The operator on the right-hand side is precisely what one obtains from integrating out a massive gauge boson. If quantum chromodynamics is embedded in a larger gauge theory, called “topcolor”, then an interaction such as that on the right side of (2.3) naturally arises. For example, suppose that the topcolor gauge symmetry is $SU(3)_1 \times SU(3)_2$, which spontaneously breaks to the diagonal subgroup. The theory contains eight massless gauge fields, the gluons, and eight gauge fields of mass M , the colorons. With appropriate gauge quantum number assignments, the exchange of a massive coloron produces the operator on the right side of (2.3) when we integrate it out. If g_{tc} is the gauge coupling constant, we identify $G \sim g_{tc}^2/M^2$.

The Pagels-Stokar relation suggests that if the scale Λ of new physics is in the TeV range, the top quark mass resulting from $SU(2)$ breaking will be unacceptably large. A solution to this difficulty [6] is to introduce a new heavy fermion, χ , a weak singlet with the same hypercharge as t_R , which participates in the breaking of electroweak symmetry. Since χ is an isosinglet, it does not contribute too much to Peskin and Takeuchi’s S parameter [3]. By comparison, in traditional technicolor models, the large number of “extra” $SU(2)$ doublets needed to construct the Higgs sector give large contributions to S that are probably unacceptable.

The introduction of the χ leads to a modification of the Pagels-Stokar relation for the top quark mass. We can derive the new relation using an effective field theory approach [10]. To begin, we assume that the gauge structure of the theory is such that the exchange of a massive coloron between ψ_L and χ_R (rather than the t_R) produces a four-fermion interaction of the form

$$\mathcal{L}' = \frac{g_{tc}^2}{M^2}(\bar{\psi}_L\chi_R)(\bar{\chi}_R\psi_L) + \dots, \quad (2.4)$$

In addition, the theory admits, after topcolor symmetry breaking, the following allowed mass terms

$$\mathcal{L}' = -\mu_{\chi\chi}\bar{\chi}_L\chi_R - \mu_{\chi t}\bar{\chi}_Lt_R + \text{h.c.} + \dots. \quad (2.5)$$

Since both χ_L and t_R are $Y = \frac{4}{3}$ singlets, these fields can mix, so we define mass eigenstates through the following rotation:

$$\begin{aligned}\chi'_R &= \cos \theta \chi_R + \sin \theta t_R \\ t'_R &= \cos \theta t_R - \sin \theta \chi_R\end{aligned}\quad \tan \theta = \frac{\mu_{\chi t}}{\mu_{\chi\chi}}. \quad (2.6)$$

The interaction Lagrangian then becomes

$$\mathcal{L}' = -\overline{m}\bar{\chi}_L\chi'_R + \text{h.c.} + \frac{g_{tc}^2}{M^2}(\bar{\psi}_L(\cos \theta \chi'_R - \sin \theta t'_R))((\cos \theta \bar{\chi}'_R - \sin \theta \bar{t}'_R)\psi_L) \quad (2.7)$$

where $\overline{m}^2 \equiv \mu_{\chi\chi}^2 + \mu_{\chi t}^2$. We can analyze the effects of the four-fermi interaction by rewriting the Lagrangian in terms of a static auxiliary Higgs field H . The interaction Lagrangian can be written as

$$\mathcal{L}' = -\overline{m}\bar{\chi}_L\chi'_R + \text{h.c.} + g_t\bar{\psi}_L(\cos \theta \chi'_R - \sin \theta t'_R)H_0 + \text{h.c.} - M^2 H_0^\dagger H_0; \quad (2.8)$$

at low energies, we shall find that H_0 plays the role of the unrenormalized Higgs doublet. For energies $\mu < \overline{m} < M$, the χ field decouples and, upon integrating it out of the theory, generates the following one loop effective Lagrangian:

$$\mathcal{L}'_{\text{eff}} = -g_t \sin \theta [\bar{\psi}_L t'_R H + \text{h.c.}] + D_\mu H^\dagger D^\mu H - m_H^2 H^\dagger H - \lambda(H^\dagger H)^2. \quad (2.9)$$

Here, H is the renormalized Higgs field, $H = \sqrt{Z_H}H_0$, and g_t is the renormalized coupling, $g_t = g_{tc}/\sqrt{Z_H}$, where the wave function renormalization induced by integrating out the χ is

$$Z_H = \frac{g_{tc}^2 N_c}{16\pi^2} \left[\ln \frac{M^2}{\overline{m}^2} + \sin^2 \theta \ln \frac{\overline{m}^2}{\mu^2} + \mathcal{O}(1) \right]. \quad (2.10)$$

The Higgs mass and self-coupling constant, in terms of the unrenormalized quantities $m_{H_0}^2 = Z_H m_H^2$ and $\lambda_0 = Z_H^2 \lambda$, are

$$\begin{aligned}m_{H_0}^2 &= M^2 - \frac{g_{tc}^2 N_c}{8\pi^2} \left[M^2 - \cos^2 \theta \overline{m}^2 \ln \frac{M^2}{\overline{m}^2} \right] + \mathcal{O}(\overline{m}^2, \mu^2) \\ \lambda_0 &= \frac{g_{tc}^2 N_c}{8\pi^2} \left[\ln \frac{M^2}{\overline{m}^2} - \sin^4 \theta \ln \frac{\overline{m}^2}{\mu^2} + \mathcal{O}(1) \right].\end{aligned} \quad (2.11)$$

Observe that for $\mu < \overline{m} < M$, H is a dynamic scalar field which has the same quantum numbers as a Higgs field. If this dynamically generated mass term becomes negative, then the Higgs acquires a vacuum expectation value. This occurs for $\cos \theta \approx 1$ when

$$\frac{g_{tc}^2 N_c}{8\pi^2} \geq \left[1 - \frac{\mu_{\chi\chi}^2}{M^2} \ln \frac{M^2}{\mu_{\chi\chi}^2} \right]^{-1}$$

where we have used

$$\overline{m}^2 = \mu_{\chi\chi}^2 + \mu_{\chi t}^2 \approx \mu_{\chi\chi}^2$$

which is appropriate for $\sin\theta \ll 1$. If we then write the Higgs vacuum expectation value in the usual form,

$$\langle H \rangle = \begin{pmatrix} v/\sqrt{2} \\ 0 \end{pmatrix} \quad v = 246 \text{ GeV}, \quad (2.12)$$

the top quark acquires a mass,

$$m_t = g_t \sin\theta \frac{v}{\sqrt{2}}. \quad (2.13)$$

The coupling g_t is related to the topcolor gauge coupling by a factor of the wave function renormalization: $g_t = g_{tc}/\sqrt{Z_H}$. When we substitute in the expression in equation (2.10) and retain only the leading term in $\sin^2\theta$, we have an expression which superficially resembles that of the bubble approximation (2.2):

$$v^2 = \frac{N_c}{8\pi^2} \frac{m_t^2}{\sin^2\theta} \ln \frac{M^2}{\overline{m}^2} + \mathcal{O}(\sin^2\theta). \quad (2.14)$$

Therefore we see that it is possible naturally to have a top quark much lighter than the 600 GeV required by the bubble approximation formula:

$$m_t = 174 \text{ GeV} \quad \frac{m_t}{\sin\theta} \sim 600 \text{ GeV}. \quad (2.15)$$

Up until now, we have made several assumptions about the relative sizes of the mass terms as well as which couplings appear in the low energy effective Lagrangian. For these to occur naturally constrains the models that we can consider. For example, equation (2.14) requires that $\sin\theta \ll 1$, or $\mu_{\chi\chi} \gg \mu_{\chi t}$, so the dynamics that produce these mass terms should naturally favor a heavier mass for the $\bar{\chi}\chi$ -term. Moreover, to produce a successful seesaw, we neglected terms containing $\bar{\psi}_L t_R$, so such terms should also be naturally suppressed. For a specific model, these restrictions on the sizes of the mass terms translate into the requirements on the relative mass dimensions of the effective operators that produce them in the higher energy theory.

By a completely analogous procedure, we could also introduce a weak singlet partner for the b -quark,

$$\omega \sim (1, -\frac{2}{3}) \quad \text{under} \quad SU(2)_W \times U(1)_Y. \quad (2.16)$$

The low energy spectrum of such a theory, which we study in section 4, contains two Higgs doublets. In models of this type, the top and bottom quark masses can be generated by

the $SU(2)$ breaking condensates $\langle \bar{t}_L \chi_R \rangle$ and $\langle \bar{b}_L \omega_R \rangle$. Of course, it is necessary to adjust the see-saw mechanism appropriately in order to get the correct b quark mass. This is different from the situation in models with only a χ -type quark. In models with only a χ , it is often necessary to “tilt” the vacuum in such a way that only t -quark condensates form; if the b condenses as well, its mass becomes too large. From this perspective, models with both χ and ω quarks have the virtue that they do not require such tilting mechanisms.

3. Constructing a Successful Topcolor Seesaw Model.

The gauge theory structure of a successful topcolor theory is of the general form

$$G \times G_{\text{tc}} \times SU(2)_W \times U(1)_Y \quad (3.1)$$

where G_{tc} is the topcolor group, usually two or more copies of $SU(3)$, that breaks down to ordinary $SU(3)_{\text{color}}$ under the influence of some additional gauge interactions with the local symmetry group G . In the simplest topcolor models, $G_{\text{tc}} = SU(3) \times SU(3)$, but we shall later study a model with three $SU(3)$ factors. The matter content of the theory should include, in addition to the standard model fields, some $SU(2)_W$ -inert fermions $\chi_{L,R}$ with hypercharge $Y = \frac{4}{3}$ (and perhaps some $Y = -\frac{2}{3}$ weak singlets for a b quark seesaw), and some fermions that break topcolor when the G gauge interactions become strong. Some additional matter fields may be required to cancel the anomalies in the theory. A realistic topcolor seesaw model must be arranged to satisfy the following properties to produce the correct low energy physics. We shall assume that the models are self-contained to the extent that they are anomaly free and do not require unspecified “spectator” fermions to cancel gauge anomalies. In addition, in a fully realistic model, it must be possible to construct higher-dimensional gauge-invariant operators that give rise to light quark and lepton masses. We assume that such operators come from integrating out new physics at a “flavor” scale Λ_f of order 50 to 100 TeV. We shall further assume that the flavor dynamics are strong. This assumption is not necessary but it is convenient since it allows us to use the tools of naïve dimensional analysis (NDA) [11] to estimate the mass scales of the effective operators that arise at energies below the scales associated with the flavor physics, f_f and Λ_f . Here f_f is the decay constant of the pions associated with flavor symmetry breaking, while $\Lambda_f \leq 4\pi f_f$ is the physical mass of the light (non-Goldstone) composite states associated with the strong flavor interactions.

The requirement that it be possible for such operators to generate quark and lepton masses of order 1 GeV can be used as a guide in building models. We also demand that all the energy scales and particle masses should arise dynamically. This condition produces a natural hierarchy of particle masses. If the masses are not protected by chiral symmetries, it is difficult to explain why they should be small compared to Λ_f .

Before stating the models we study here, we shall present several simpler models since it is instructive to see how these fail. The models are represented in “Moose notation” [12], which efficiently encodes the gauge transformation properties of the matter fields and allows us quickly to write anomaly-free models. In the Moose notation, the $SU(N)$ gauge groups are represented by circles while fermions are lines. A fermion line emerging from an $SU(N)$ group lives in the N -representation if left-handed (\bar{N} if right-handed) while an entering fermion line lives in the \bar{N} -representation if left-handed (N if right-handed).

One might hope to succeed with a seesaw model involving a single group mediating between the two $SU(3)$ ’s that compose the topcolor group. An example of such a theory is shown in figure 1. In this model, the $SU(4)$ group can break the $SU(3) \times SU(3)$ symmetry dynamically. In particular, if the $SU(4)$ is more strongly coupled than the $SU(3)$ interactions, we expect the ξ quarks to condense in the $\bar{\xi}_L \xi_R$ channel. This condensate transforms as $(3, \bar{3})$ under $SU(3) \times SU(3)$ and therefore can break the $SU(3)$ factors down to their diagonal $SU(3)$ subgroup. Notice that the light fermions—the χ , ω , and standard model fields—are anomalous under $SU(3) \times SU(3)$. By choosing the group $SU(4)$ for the interactions that break topcolor, the $\xi_{L,R}$ fields cancel the topcolor anomalies. To protect the light quark masses, we have chosen the left- and right-hand fields to transform under different $SU(3)$ groups. In this model, the third generation is distinguished as follows: we can choose t_R and b_R to be respectively the linear combinations of U_R^i and D_R^i quarks that couple to the χ_L and ω_L fermions. The left-handed ψ_L^3 fields are defined by the linear combination of the ψ_L^i fields that couples to the Higgs field that develops a vacuum expectation value. It is not clear, however, that prohibitively large flavor changing neutral currents do not arise in this model.

The light quark masses arise from operators such as

$$\frac{1}{\Lambda_f f_f^4} (\bar{\psi}_L^3 \chi_R) (\bar{U}_R^1 \xi_L) (\bar{\xi}_R \psi_L^1). \quad (3.2)$$

When the $SU(4)$ interactions cause the $\bar{\xi}_R \xi_L$ condensate to form and break $SU(3) \times SU(3) \rightarrow SU(3)_{\text{QCD}}$, the naïve estimate for the a light quark mass is

$$m_u \sim \frac{\langle \bar{\xi}_R \xi_L \rangle}{\Lambda_f f_f^4} \langle \bar{\psi}_L^3 \chi_R \rangle. \quad (3.3)$$

$\langle \bar{\xi}_R \xi_L \rangle$ is the vacuum expectation value of the $\bar{\xi}_R \xi_L$ condensate which is of the order $\langle \bar{\xi}_R \xi_L \rangle \sim f_{tc}^2 \Lambda_{tc}$, using the rules of naïve dimensional analysis [11]. Here f_{tc} and Λ_{tc} play the analogous roles for the strongly interacting topcolor dynamics as f_f and Λ_f played in the flavor physics. In terms of the coloron mass M introduced in section 2, we have $M \sim \Lambda_{tc} \leq 4\pi f_{tc}$. One of the difficulties with this model is that lepton masses can arise from dimension six operators,

$$\epsilon_{ab}(\bar{\psi}_L^a \chi_R)(\bar{\ell}_L^b e_R) \quad (3.4)$$

and should be generically heavier than the quark masses by a factor $\Lambda_f f_f^2 / \langle \bar{\xi}_R \xi_L \rangle$. For example, when the scale of the flavor physics is $f_f \sim 100 \text{ TeV}$ and $f_{tc} \sim 10 \text{ TeV}$, this factor is $\mathcal{O}(10^3)$ which is unacceptably large. Another difficulty for models with $G_{tc} = SU(3) \times SU(3)$ is that no symmetry prevents a $\bar{\chi}_L t_R$ (or even a $\bar{\chi}_L U_R^i$) mass term from arising. Such a term could spoil the seesaw mechanism since there is no reason that it could not have a mass of the order of the flavor scale physics. This observation suggests that the fields χ_L , t_R and χ_R should transform under different $SU(3)$ groups. Here, we shall attempt to construct models which do not admit these tree-level mass terms—a condition which will lead us to consider models with more complicated gauge symmetries. Yet the simplicity of this linear Moose model is so enticing that we shall explore models similar to it elsewhere [13].

A model with three $SU(3)$ topcolor factors contains enough symmetry to prevent the $\bar{\chi}_L t_R$ or $\bar{\chi}_R \chi_L$ terms from forming at too high an energy scale. One such model of this form is shown in figure 2 where the dimensions of the $SU(m)$ groups that break topcolor have been chosen to cancel any anomalies. Unfortunately, in this model the $\bar{\chi}_L t_R$ mass term originates from a dimension nine operator:

$$\frac{\Lambda_f}{f_f^6}(\bar{\chi}_L \xi_R)(\bar{\xi}_L \zeta_R)(\bar{\zeta}_L t_R) \rightarrow \frac{\Lambda_f \langle \bar{\xi}_L \xi_R \rangle \langle \bar{\zeta}_L \zeta_R \rangle}{f_f^6} \bar{\chi}_L t_R \sim \frac{\Lambda_f \Lambda_{tc}^2 f_{tc}^4}{f_f^6} \bar{\chi}_L t_R \quad (\text{NDA}) \quad (3.5)$$

which is probably too small unless the ratio of the flavor scale to the topcolor scale is only about a factor of three. This difficulty comes from the need to straddle the entire diagram to produce an operator containing χ_L and t_R that is invariant under all of the gauge symmetries. The remedy is to add another gauge group which links the two ends. Thus we are led to consider topcolor models such as that of figure 3 which was first proposed in [10].

With only a single additional ($Y = \frac{4}{3}$) fermion, this model produces a single Higgs $SU(2)_W$ doublet in the low energy theory. An unpleasant feature of this model is that

it still requires some mechanism to tilt the vacuum to prevent the formation of a large $\bar{b}_R \psi_L^3$ condensate which would produce an unacceptably large b quark mass [10]. Figure 4 shows a model with two additional fermions, χ ($Y = \frac{4}{3}$) and ω ($Y = -\frac{2}{3}$), which act like a weak-inert fourth generation and avoid this need for tilting. At low energies, this model contains two Higgs doublets corresponding to the $\bar{\psi}_L^3 \chi_R$ and $\bar{\psi}_L^3 \omega_R$ condensates. The b quark mass participates in its own seesaw so that it is possible to have $m_\omega \sim 10 \text{ TeV}$ with $m_b \sim 4 \text{ GeV}$.

To summarize, the desire to achieve an anomaly-free model that yields a realistic low energy theory through operators of the appropriate mass dimension has led us to consider models with a rather rich gauge group structure. We shall focus in particular upon the two models shown in figures 3 and 4 but any topcolor model with a single $Y = \frac{4}{3}$ fermion or a $Y = (\frac{4}{3}, -\frac{2}{3})$ pair should share the same general behavior of two triangular models above, in particular the bounds on the masses of these fermions set by $Z \rightarrow b\bar{b}$ and the ρ parameter discussed below. Models with more $SU(2)_W$ singlet fermions, to a first approximation, lead to multiple copies of the Higgs fields of these two models which generically should reinforce the perturbations to R_b and $\delta\rho$. Some of our assumptions may be relaxed to obtain simpler models but only at the cost of the naturalness of the mass scales.

4. The Higgs Potential.

Now that we have a pair of models that produce a top quark seesaw, we would like to study their phenomenology in some detail. The effective potential for the one-doublet model has been carefully studied before [10] so in this section we concentrate on the two-doublet model and derive its Higgs spectrum. A few points deserve special attention. First, in the leading approximation, the two doublet model preserves a global Peccei-Quinn $U(1)$ symmetry, so it has an unacceptable weak scale axion. We shall add explicit, but small, Peccei-Quinn breaking terms to give this “axion” a mass. Second, We shall make some simplifying assumptions about the dependence of the low energy theory on m_χ and m_ω . When $m_\chi = m_\omega$, the model has a custodial $SU(2)_R$ symmetry which is reflected in the Higgs spectrum: both Higgs doublets acquire equal vacuum expectation values, and the scalars are grouped into custodial $SU(2)$ multiplets. We shall assume that this behavior persists for $m_\chi \neq m_\omega$, provided that both are light compared to the topcolor scale. We will return elsewhere to the study of custodial $SU(2)$ breaking by m_χ and m_ω .

We shall use the techniques of [5], [6] to study the low energy Higgs spectrum. These methods are equivalent to the NJL approximation [14], which is sufficient for our purposes.

In the two doublet model, the leading-order four-fermion interaction in $1/N_c$,

$$\mathcal{L}_{\text{int}} = \frac{g_{\text{tc}}^2}{M^2} [(\bar{\psi}_L \chi_R)(\bar{\chi}_R \psi_L) + (\bar{\psi}_L \omega_R)(\bar{\omega}_R \psi_L)] + \dots, \quad (4.1)$$

comes from the Fierz rearrangement of the operator corresponding to the exchange of a massive coloron between the ψ_L and the χ_R or ω_R currents. Other operators, such as those originating from LL and RR currents are suppressed in the $1/N_c \rightarrow 0$ limit. This interaction preserves a Peccei-Quinn symmetry. In order to give the “axion” an acceptable mass, we add an explicit breaking term to the Lagrangian:

$$\begin{aligned} \mathcal{L}_{\text{int}} = & \frac{g_{\text{tc}}^2}{M^2} [(\bar{\psi}_L \chi_R)(\bar{\chi}_R \psi_L) + (\bar{\psi}_L \omega_R)(\bar{\omega}_R \psi_L)] \\ & + \xi \frac{g_{\text{tc}}^2}{M^2} [\epsilon_{ab}(\bar{\psi}_L^a \chi_R)(\bar{\psi}_L^b \omega_R) + \epsilon^{ab}(\bar{\chi}_R \psi_{aL})(\bar{\omega}_R \psi_{bL})] + \dots. \end{aligned} \quad (4.2)$$

Here ϵ^{ab} is completely antisymmetric with $\epsilon^{12} = -\epsilon^{21} = 1$. We should point out that the Peccei-Quinn term we have added is only one of many possible terms that could arise from the higher energy flavor physics. We expect that this term should be small compared to (4.1), which translates into the requirement $\xi \ll 1$. This follows from the fact that interactions originating from the flavor physics are typically suppressed by the ratio of the topcolor scale (~ 10 TeV) to the flavor scale (~ 100 TeV). We shall show that both these conditions can be simultaneously met—that it is possible to have ξ small and the mass of the light pseudoscalar Higgs well above current experimental bounds.

If we combine the χ_R and ω_R fields into a doublet,

$$\lambda_R \equiv \begin{pmatrix} \chi_R \\ \omega_R \end{pmatrix} \quad (4.3)$$

then the interaction Lagrangian becomes

$$\mathcal{L}_{\text{int}} = \frac{g_{\text{tc}}^2}{M^2} (\bar{\psi}_{aL} \lambda_R^b) (\bar{\lambda}_{bR} \psi_L^a) + \frac{\xi}{2} \frac{g_{\text{tc}}^2}{M^2} [\epsilon^{ab} \epsilon_{cd} (\bar{\psi}_{aL} \lambda_R^c) (\bar{\psi}_{bL} \lambda_R^d) + \epsilon^{ab} \epsilon_{cd} (\bar{\lambda}_{aR} \psi_L^c) (\bar{\lambda}_{bR} \psi_L^d)]. \quad (4.4)$$

We next introduce a static, auxiliary field \mathcal{M}_b^a , which becomes a pair of Higgs doublets in the low energy effective theory once we have integrated out the heavy χ and ω fermions. We introduce \mathcal{M} through the effective Lagrangian

$$\begin{aligned} \mathcal{L}_{\text{eff}} = & g_{\text{tc}} \left[\bar{\psi}_{aL} \mathcal{M}_b^a \lambda_R^b + \bar{\lambda}_{aR} \mathcal{M}_b^{\dagger a} \psi_L^b + \xi \bar{\lambda}_{aR} \tilde{\mathcal{M}}_b^a \psi_L^b + \xi \bar{\psi}_{aL} \tilde{\mathcal{M}}_b^{\dagger a} \lambda_R^b \right] \\ & - M^2 \left[\text{Tr}(\mathcal{M}^\dagger \mathcal{M}) + \frac{1}{2} \xi \text{Tr}(\tilde{\mathcal{M}} \mathcal{M}) + \frac{1}{2} \xi \text{Tr}(\tilde{\mathcal{M}}^\dagger \mathcal{M}^\dagger) \right]. \end{aligned} \quad (4.5)$$

Note that the equations of motion for this static field,

$$\begin{aligned}\mathcal{M}_a^b &= \frac{g_{tc}}{M^2} \bar{\psi}_{aL} \lambda_R^b \\ \tilde{\mathcal{M}}_a^b &= \frac{g_{tc}}{M^2} \epsilon^{bc} \bar{\psi}_{cL} \lambda_R^d \epsilon_{da} = \epsilon^{bc} \mathcal{M}_c^d \epsilon_{da},\end{aligned}\tag{4.6}$$

when substituted back into the effective Lagrangian, reproduce the original interaction Lagrangian, (4.4). In the low energy theory, we should integrate out the heavy degrees of freedom, which promotes the auxiliary static field to a fully dynamic Higgs field. To one-loop order, this procedure produces a propagating, self-interacting Higgs field—working to first order in ξ , we find

$$\begin{aligned}\mathcal{L}_{1\text{-loop}} &= Z_\phi \text{Tr}(\partial_\mu \mathcal{M}^\dagger \partial^\mu \mathcal{M}) + \xi Z_\phi \left[\text{Tr}(\partial_\mu \tilde{\mathcal{M}} \partial^\mu \mathcal{M}) + \text{h.c.} \right] \\ &\quad + Z_m \text{Tr}(\mathcal{M}^\dagger \mathcal{M}) + \xi \left[Z_m \text{Tr}(\tilde{\mathcal{M}} \mathcal{M}) + \text{h.c.} \right] \\ &\quad - M^2 \left[\text{Tr}(\mathcal{M}^\dagger \mathcal{M}) + \frac{1}{2} \xi \text{Tr}(\tilde{\mathcal{M}} \mathcal{M}) + \frac{1}{2} \xi \text{Tr}(\tilde{\mathcal{M}}^\dagger \mathcal{M}^\dagger) \right] \\ &\quad - \lambda \left[\text{Tr}(\mathcal{M}^\dagger \mathcal{M} \mathcal{M}^\dagger \mathcal{M}) + \xi \left[\text{Tr}(\mathcal{M}^\dagger \mathcal{M}) \text{Tr}(\tilde{\mathcal{M}} \mathcal{M}) + \text{h.c.} \right] \right].\end{aligned}\tag{4.7}$$

where

$$\begin{aligned}Z_\phi &\equiv \frac{g_{tc}^2 N_c}{(4\pi)^2} \ln \frac{M^2}{\mu^2} \\ Z_m &\equiv \frac{2g_{tc}^2 N_c}{(4\pi)^2} (M^2 - \mu^2) \\ \lambda &\equiv \frac{g_{tc}^4 N_c}{(4\pi)^2} \ln \frac{M^2}{\mu^2}.\end{aligned}\tag{4.8}$$

Observe that at energies $\mu < M$, below the scale at which the effective field theory description breaks down, we have a fully dynamic Higgs field; at the boundary, $\mu = M$, the one-loop effects that produce these dynamics are small.

We next evaluate the Higgs spectrum in the two-doublet model by expanding the fields about the vacuum,¹

$$\mathcal{M} = \frac{v}{\sqrt{2}} \begin{pmatrix} 1 & 0 \\ 0 & 1 \end{pmatrix} \quad \text{for } v = 246 \text{ GeV}/\sqrt{2} = 174 \text{ GeV}.\tag{4.9}$$

The fact that the two entries on the diagonal are equal is a consequence of the $\mathcal{M} \leftrightarrow -\tilde{\mathcal{M}}$ symmetry of the Lagrangian, which we have checked is left unbroken by the vacuum. If

¹ This corresponds to the case $\tan \beta = 1$ in the notation of [15].

we define the fields representing fluctuations about this vacuum state by

$$\begin{aligned}
\mathcal{M}_1^1 &= \frac{1}{\sqrt{2}} (v + H^0 + h^0 + iA^0 + iG^0) \\
\mathcal{M}_2^1 &= \frac{1}{\sqrt{2}} (H^+ - G^+) \\
\mathcal{M}_1^2 &= \frac{1}{\sqrt{2}} (H^- + G^-) \\
\mathcal{M}_2^2 &= \frac{1}{\sqrt{2}} (v + H^0 - h^0 + iA^0 - iG^0),
\end{aligned} \tag{4.10}$$

then we find that the fields G^0, G^\pm are the Goldstone bosons associated with the $SU(2)_W \times U(1)_Y \rightarrow U(1)_{\text{em}}$ symmetry breaking while the others represent a pair of neutral Higgs fields, h^0 and H^0 , a charged Higgs field H^\pm , and a neutral pseudoscalar Higgs field, A^0 . In the usual notation for two doublet models [15], these linear combinations correspond to mixing angles $\alpha = -\pi/4$ and $\beta = \pi/4$. To leading order in the parameter ξ , inserting the values from equation (4.7) and canonically normalizing the fields, we find that the masses of the h^0, H^0 and H^\pm are degenerate,

$$m_{h^0}^2 = m_{H^0}^2 = m_{H^\pm}^2 \equiv m_H^2 = \frac{2v^2\lambda_1}{Z_\phi^2} = \frac{32\pi^2 g_{\text{tc}}^2 v^2}{N_c \ln(M^2/\mu^2)}. \tag{4.11}$$

The pseudoscalar Higgs has a mass scaled down by a factor $\sqrt{2\xi}$,

$$m_{A^0}^2 = 2\xi m_H^2. \tag{4.12}$$

The current lower bound on the mass of a pseudoscalar Higgs is about 62 GeV [16], so that for $m_H \sim 1$ TeV, even a small amount of Peccei-Quinn symmetry breaking, larger than $\xi \sim 1/500$, is sufficient to be in accord with observations. Such a value of ξ could easily be generated by physics at the flavor scale; if this scale is an order of magnitude above the scale at which topcolor breaks, we might expect $\xi \sim 10^{-2}$.

5. Experimental Constraints on Topcolor Models.

Most of the new physics in a topcolor model appears at scales of 1–10 TeV or higher, so that the new fields, whether the heavy fermions or the extra Higgs fields, can not be directly seen in current experiments. However, their presence should appear in precise tests of the electroweak theory, particularly in measurements of the ρ parameter or R_b , the ratio of decay width of $Z \rightarrow b\bar{b}$ to that of $Z \rightarrow \text{hadrons}$. In the one-doublet model, we use the effect of the new heavy fermion on Peskin and Takeuchi's [3] T parameter combined

with the Higgs's contribution to S and T to map out the experimentally allowed region of the $m_{\text{higgs}}-m_\chi$ plane. The allowed χ mass depends on the mass of the Higgs, but for a 0.5–1 TeV Higgs, the 90% confidence level limits place m_χ between about 5–8 TeV. In the two-doublet model, the limits on R_b exclude an ω mass less than about 12 TeV. The mass of the χ is not so tightly constrained. Again, determining the contributions of the new physics, the χ , ω and new Higgs fields, to S and T , we plot the allowed regions in the $m_\chi-m_\omega$ planes for different choices of the Higgs fields' masses.

To generate these plots for the allowed masses, we must first determine how the new fermions contribute to T . As mentioned in the introduction, one of the advantages of choosing χ and ω to be weak singlets is that they do not then contribute significantly to S . We could analyze $T = \alpha_{\text{QED}} \delta\rho \equiv \alpha_{\text{QED}} (\rho - \rho_{\text{sm}})^2$ by summing the one-loop vacuum polarization graphs for the Z^0 and W^\pm propagators that contain χ and t fermion loops to find,

$$\delta\rho = \frac{N_c}{16\pi^2 v^2} \left[\sin^4 \theta_L^\chi m_\chi^2 + 2 \sin^2 \theta_L^\chi \cos^2 \theta_L^\chi \frac{m_\chi^2 m_t^2}{m_\chi^2 - m_t^2} \ln \frac{m_\chi^2}{m_t^2} - \sin^2 \theta_L^\chi (2 - \sin^2 \theta_L^\chi) m_t^2 \right] \quad (5.1)$$

for the one-doublet theory and, including the ω and b loops as well,

$$\begin{aligned} \delta\rho = \frac{N_c}{16\pi^2 v^2} & \left[\sin^4 \theta_L^\chi f(m_\chi, m_t) + \sin^4 \theta_L^\omega f(m_\omega, m_b) \right. \\ & + \sin^2 \theta_L^\chi (f(m_\chi, m_b) - f(m_t, m_b) - f(m_\chi, m_t)) \\ & + \sin^2 \theta_L^\omega (f(m_\omega, m_t) - f(m_t, m_b) - f(m_\omega, m_b)) \\ & \left. + \sin^2 \theta_L^\chi \sin^2 \theta_L^\omega (f(m_\chi, m_\omega) + f(m_t, m_b) - f(m_\omega, m_t) - f(m_\chi, m_b)) \right] \end{aligned} \quad (5.2)$$

for the two-doublet theory, where

$$f(m_1, m_2) = m_1^2 + m_2^2 - \frac{2m_1^2 m_2^2}{m_1^2 - m_2^2} \ln \frac{m_1^2}{m_2^2}. \quad (5.3)$$

Notice that $f(m_1, m_2)$ vanishes when $m_1 = m_2$. Also, θ_L^χ is the mixing angle between χ_L and t_L that rotates these states into the mass eigenstate basis, and similarly for θ_R^χ , $\theta_{L,R}^\omega$.

The calculations which led to these results are lengthy and provide little insight into the physics so we shall extract the leading behavior via an effective operator approach, described in [17]. Our calculations in this section do not include effects of the Peccei-Quinn symmetry breaking term in (4.2). We showed that these effects could be small

² Here ρ_{sm} is the standard model prediction to the ρ parameter.

and still produce a mass for the pseudoscalar Higgs, and moreover we expect them to be small when they originate from the flavor physics since such effects are generically suppressed by powers of the ratio of the topcolor scale to the flavor scale. It is important, however, that $\tan \beta \equiv v_2/v_1 \approx 1$, where $v_{1,2}$ are the vacuum expectation values for the two Higgs doublets, since when the custodial $SU(2)$ symmetry in the Higgs sector is broken, $\delta\rho$ receives potentially large corrections that scale quadratically in the Higgs masses [18]. However, we have explicitly checked that $\tan \beta = 1$ is the minimum of the $\xi = 0$ vacuum so we set $\tan \beta = 1$ in the following calculation for the two-doublet model.

5.1. The One-Doublet Model.

Generically, the presence of new physics at some high energy scale $M \gg v$ appears at low energies in the form of non-renormalizable corrections to the standard model. Since these non-renormalizable operators arise when we integrate out the heavy fields, they enter the low energy theory suppressed by powers of $1/M$. We can use the effective operator approach of [17] and [19] to estimate the corrections to $\delta\rho$ due to integrating out the χ and ω fields, so that the relevant mass scale for M is m_χ or m_ω . The operators that produce the leading contribution to $\delta\rho$ involve four Higgs fields, at most two derivatives and must break the custodial $SU(2)$ symmetry. The only such operator is³

$$\frac{c_4}{m_\chi^2} \mathcal{O}_4 = \frac{c_4}{m_\chi^2} (H_a^\dagger D_\mu H^a) (H_b^\dagger D^\mu H^b) + \text{h.c.} \quad (5.4)$$

More generally, a one-loop graph in the full theory will contain custodial $SU(2)$ -conserving parts as well; these can contribute to the effective operators

$$\frac{c_5}{m_\chi^2} \mathcal{O}_5 = \frac{c_5}{m_\chi^2} (H_a^\dagger D^2 H^a) (H_b^\dagger H^b) + \text{h.c.} \quad \frac{c_6}{m_\chi^2} \mathcal{O}_6 = \frac{c_6}{m_\chi^2} (D_\mu H_a^\dagger D^\mu H^a) (H_b^\dagger H^b). \quad (5.5)$$

Let us first determine the matching contribution to \mathcal{O}_4 in the one Higgs doublet model which comes from the one-loop diagram in figure 5. Expanding this graph in powers of the external momenta and retaining the quadratic terms, we find

$$\cdots - \frac{N_c}{16\pi^2} \delta_d^a \delta_b^c g_{tc}^4 \cos^4 \theta_L^\chi \cos^4 \theta_R^\chi \left[\frac{1}{12} \frac{1}{m_\chi^2} [3s + 9t + u] \right] + \delta_b^a \delta_d^c (s \leftrightarrow u) \cdots \quad (5.6)$$

³ Here we have labeled the operator to agree with the notation in [17].

where s , t and u are the usual Mandelstam variables. Matching this to the effective theory, equations (5.4) and (5.5),

$$\frac{i}{m_\chi^2} \delta_d^a \delta_b^c \left(c_4 \frac{1}{2} (t - s - u) + c_5 (s + t + u) + c_6 \frac{1}{2} (u - s - t) \right) + \frac{i}{m_\chi^2} \delta_b^a \delta_d^c (s \leftrightarrow u) \quad (5.7)$$

we discover that the custodial $SU(2)$ violating piece is

$$c_4 = -\frac{N_c}{16\pi^2} \frac{g_{tc}^4}{4}, \quad (5.8)$$

upon taking $\theta_L^\chi \approx 0 \approx \theta_R^\chi$, which we require for the top quark seesaw. This leads to a shift in the ρ parameter of [17],

$$\delta\rho = -c_4 \frac{v^2}{m_\chi^2} = \frac{N_c}{16\pi^2} \frac{g_{tc}^4}{4} \frac{v^2}{m_\chi^2}, \quad (5.9)$$

which agrees with the leading piece of the result of the exact, but much lengthier, analysis of the one-loop vacuum polarization diagrams of equation (5.1).

A second, logarithmic, contribution to $\delta\rho$ arises from running from $\mu = m_\chi$ down to m_t . In the theory below the scale of the heavy fermions, integrating out the χ produces an effective operator of the form,

$$\mathcal{O} = \frac{g_{tc}^2}{m_\chi^2} (\bar{\psi}_{La}^3 H^a) \gamma^\mu D_\mu (H_b^\dagger \psi_L^{3b}). \quad (5.10)$$

When inserted into the diagrams shown in figure 6 (there represented by a heavy dot), the piece of these diagrams which is quadratic in the momenta (λ_t is the top quark Yukawa coupling),

$$-\frac{N_c}{16\pi^2} \frac{\lambda_t^2 g_{tc}^2}{2} \frac{\mu^\epsilon}{\epsilon} \delta_d^a \delta_b^c [s + 3t - u] + \dots, \quad (5.11)$$

produces a contribution to c_4 given by,

$$-\frac{N_c}{16\pi^2} \frac{\lambda_t^2 g_{tc}^2}{2} \ln \mu^2 + \dots \quad (5.12)$$

Running between m_χ and m_t gives a logarithmic correction to the matching term found before, so that

$$\delta\rho = \frac{N_c}{16\pi^2} \frac{g_{tc}^4}{4} \frac{v^2}{m_\chi^2} \left[1 + 2 \frac{\lambda_t^2}{g_{tc}^2} \ln \frac{m_\chi^2}{m_t^2} \right], \quad (5.13)$$

which agrees with the corresponding leading terms of the exact analysis to leading order in θ^χ . To see this, recall that $\theta^\chi \simeq \lambda_t/g_{tc}$ for small $\lambda_t \ll g_{tc}$.

The allowed values for the χ mass for a range of Higgs masses are summarized in figure 7. In this figure we have shown the regions in the $m_{\text{higgs}}-m_\chi$ plane which agree with the latest set of precision electroweak tests [1] to within a 68% and a 90% confidence level. The Higgs field makes its own contribution to the S and T (or $\rho = \alpha_{\text{QED}} T$) parameters through [3]

$$\begin{aligned} S_{\text{higgs}} &\approx \frac{1}{12\pi} \ln \frac{m_{\text{higgs}}^2}{m_{\text{higgs, ref}}^2} \\ T_{\text{higgs}} &\approx -\frac{3}{16\pi \cos^2 \theta_W} \ln \frac{m_{\text{higgs}}^2}{m_{\text{higgs, ref}}^2}, \end{aligned} \tag{5.14}$$

where the reference Higgs mass was chosen to be $m_{\text{higgs, ref}} = 300 \text{ GeV}$. This reference mass was also used in the ZFITTER [20] routine to obtain the Standard model estimates of the electroweak parameters used to generate figure 7. The plot essentially involves only two parameters, m_{higgs} and m_χ . Therefore, we have used the 68% and 90% confidence levels for two degrees of freedom and added these to the best fit value, $\chi^2 = 21$, which occurs for $m_{\text{higgs}} = 159 \text{ GeV}$ and $m_\chi \rightarrow \infty$. This procedure actually provides a conservative estimate for the allowed region. If we use instead the 68% and 90% confidence levels appropriate for the 19 parameters used to generate the standard model contributions to figure 7, the allowed region expands slightly although the qualitative shape remains unaltered. In any event, for a relatively heavy Higgs field, 0.5–1.0 TeV, the mass of the χ fermion should lie between 5 and 8 TeV.

Notice that as the χ mass grows large and its contribution to $T = \alpha_{\text{QED}}^{-1} \delta\rho$ diminishes, the acceptable values for m_{higgs} approach the usual range quoted in [21]; for example, we find that to the 90% confidence level the mass range which best fits the current electroweak data [1] for $m_\chi \rightarrow \infty$ is

$$m_{\text{higgs}} = 159_{-56}^{+86} \text{ GeV}. \tag{5.15}$$

The presence of a heavy fermion with a mass of 5–10 TeV completely alters these bounds, which do not include the effects of the new physics, so that the Higgs can be as heavy as a $\mathcal{O}(1 \text{ TeV})$ while S and T still lie within the 90% confidence level region. We should point out that this best fit value for the Higgs is larger than the 76 GeV quoted in [1]. This difference can be explained by our choice of $\alpha_s(M_Z) = 0.118$ and $m_{\text{top}} = 173.8 \text{ GeV}$ as inputs for ZFITTER rather than the values $\alpha_s(M_Z) = 0.119$ and $m_{\text{top}} = 171.1 \text{ GeV}$ listed in table 32 of [1], and by the fact that we are including only the leading logarithmic dependence on the Higgs mass. This is a rather poor approximation for small Higgs masses, but since our fits generally favor a heavy Higgs, it is sufficient for our purposes.

5.2. The Two-Doublet Model.

Since the Higgs and its mass have yet to be observed, the precision electroweak data do not sharply constrain the masses of the new fermions in the two-doublet model. The current measurements set lower bounds of about 2.5 TeV for the χ fermion and about 12 TeV for the ω . The reason for the higher bound on the ω mass is that through mixing with the b quark, it directly affects the prediction for R_b which has been precisely measured at LEP and SLD. In contrast, the χ mass affects the T parameter along with the ω and Higgs masses so that the experimental bounds on m_χ depend greatly upon the particular values of the ω mass and the mass of the Higgs fields. Paralleling our discussion for the one-doublet model, we first develop an effective operator description for the contributions to $\delta\rho$. In the limit that the Peccei-Quinn breaking terms are small, the vacuum expectation values of the two Higgs fields are equal, so we perform our analysis with $\tan\beta = 1$. Operators that could arise from the flavor-scale physics can generically perturb the vacuum away from $\tan\beta = 1$, but since such effects depend on the details of the flavor physics, we only briefly consider $\delta\rho$ for $\tan\beta \neq 1$ without attempting to estimate β . After deriving the matching and running contributions to $\delta\rho$, we derive a more stringent bound on the ω mass by studying $Z \rightarrow b\bar{b}$.

As in the one-doublet model, we can write down the relevant dimension-six custodial SU(2) violating operators,

$$\begin{aligned}\mathcal{O}_4^\chi &= c_4^\chi (H_\chi^\dagger D_\mu H_\chi)(H_\chi^\dagger D^\mu H_\chi) \\ \mathcal{O}_4^\omega &= c_4^\omega (H_\omega^\dagger D_\mu H_\omega)(H_\omega^\dagger D^\mu H_\omega) \\ \mathcal{O}_4^{\chi\omega} &= c_4^{\chi\omega} [(H_\omega^\dagger D_\mu H_\chi)(H_\chi^\dagger D^\mu H_\omega) + \text{h.c.}].\end{aligned}\tag{5.16}$$

where $H_\chi^a = \mathcal{M}_1^a$ and $H_\omega^a = \mathcal{M}_2^a$, in terms of our earlier matrix notation.⁴ The first two operators are of the same form encountered in the one-doublet model, so we can simply write down the one-loop matching contributions:

$$c_4^\chi = -\frac{N_c}{16\pi^2} \frac{g_{\text{tc}}^4}{4} \frac{1}{m_\chi^2} \quad \text{and} \quad c_4^\omega = -\frac{N_c}{16\pi^2} \frac{g_{\text{tc}}^4}{4} \frac{1}{m_\omega^2}.\tag{5.17}$$

The third operator in equation (5.16) partially undoes the effects of the first two when $m_\chi \approx m_\omega$. The leading contribution to $\mathcal{O}_4^{\chi\omega}$ from the full theory originates in the graph shown in figure 8. Just as in the one-doublet case, we must take care to extract only the

⁴ We are neglecting the Peccei-Quinn breaking terms which are small ($\xi = 0$).

custodial- $SU(2)$ violating part of this graph. In addition to $\mathcal{O}_4^{\chi\omega}$, we can also write the following dimension-six operators that contain two derivatives and two factors of both H_χ and H_ω :

$$\begin{aligned} c_5^{\chi\omega} & [(H_\omega^\dagger D^2 H_\chi)(H_\chi^\dagger H_\omega) + \text{h.c.}] \\ \tilde{c}_5^{\chi\omega} & [(H_\omega^\dagger H_\chi)(H_\chi^\dagger D^2 H_\omega) + \text{h.c.}] \\ c_6^{\chi\omega} & [(D_\mu H_\omega^\dagger D^\mu H_\chi)(H_\chi^\dagger H_\omega) + \text{h.c.}], \end{aligned} \quad (5.18)$$

which describe a complete set up to integrations by parts. Retaining just the $SU(2)$ violating piece, we find that

$$c_4^{\chi\omega} = -\frac{N_c}{16\pi^2} \frac{g_{\text{tc}}^4}{4} \frac{2}{m_\chi^2 - m_\omega^2} \ln \frac{m_\chi^2}{m_\omega^2}. \quad (5.19)$$

The net matching contribution for the ρ -parameter due to the presence of the heavy fermions is

$$\begin{aligned} \delta\rho & = -(c_4^\chi + c_4^\omega - c_4^{\chi\omega})v^2 \\ & = \frac{N_c}{16\pi^2} \frac{g_{\text{tc}}^4 v^2}{4} \left[\frac{1}{m_\chi^2} + \frac{1}{m_\omega^2} - \frac{2}{m_\chi^2 - m_\omega^2} \ln \frac{m_\chi^2}{m_\omega^2} \right]. \end{aligned} \quad (5.20)$$

Note that the operator $\mathcal{O}_4^{\chi\omega}$ contributes to $\delta\rho$ with the opposite sign of \mathcal{O}_4^χ and \mathcal{O}_4^ω . The origin of this sign can be seen when we write the vacuum expectation values for the two Higgs fields as $\langle H_\chi \rangle = \begin{pmatrix} v \\ 0 \end{pmatrix}$ and $\langle H_\omega \rangle = \begin{pmatrix} 0 \\ v \end{pmatrix}$, where $v = 246 \text{ GeV}/2 = 123 \text{ GeV}$. Then both \mathcal{O}_4^χ and \mathcal{O}_4^ω shift the Z mass but leave the W mass unaffected while $\mathcal{O}_4^{\chi\omega}$ produces the opposite effect—it shifts the W mass while leaving the Z mass unaltered.

After matching the full and effective theories at energies $\mu \approx m_\chi, m_\omega$, $\delta\rho$ receives further logarithmic terms from running down to energies, $\mu \approx m_t, m_b$. The diagrams that produce these running contributions involve insertions of the operators

$$\frac{g_{\text{tc}}^2}{m_\chi^2} (\bar{\psi}_L H_\chi) \not{D} (H_\chi^\dagger \psi_L) + \frac{g_{\text{tc}}^2}{m_\omega^2} (\bar{\psi}_L H_\omega) \not{D} (H_\omega^\dagger \psi_L), \quad (5.21)$$

and resemble those encountered before for the one-doublet model, in figure 6. Including these logarithmic corrections, we find the following form for $\delta\rho$:

$$\begin{aligned} \delta\rho & = \frac{N_c}{16\pi^2} \frac{g_{\text{tc}}^4 v^2}{4} \left[\frac{1}{m_\chi^2} + \frac{1}{m_\omega^2} - \frac{2}{m_\chi^2 - m_\omega^2} \ln \frac{m_\chi^2}{m_\omega^2} \right. \\ & \quad \left. + \frac{\lambda_t^2}{g_{\text{tc}}^2} \frac{2}{m_\chi^2} \ln \frac{m_\chi^2}{m_t^2} + \frac{\lambda_b^2}{g_{\text{tc}}^2} \frac{2}{m_\omega^2} \ln \frac{m_\omega^2}{m_b^2} - \frac{\lambda_b^2}{g_{\text{tc}}^2} \frac{2}{m_\chi^2} \ln \frac{m_\chi^2}{m_b^2} - \frac{\lambda_t^2}{g_{\text{tc}}^2} \frac{2}{m_\omega^2} \ln \frac{m_\omega^2}{m_t^2} \right] \end{aligned} \quad (5.22)$$

which reproduces the leading terms from the analysis (5.2) of the vacuum polarization graphs of the two Higgs doublet model. Observe that in the limit $m_\chi \rightarrow m_\omega$ that $\delta\rho \rightarrow 0$.

To complete our discussion of contributions to $\delta\rho$, we briefly examine the case when $\tan\beta \neq 1$. Previously, we have assumed that the vacuum expectation values for the two Higgs doublets were of equal magnitude. If effects arising from the flavor physics break this equality, then we could have

$$\langle H_\chi \rangle = \begin{pmatrix} v_1 \\ 0 \end{pmatrix} \quad \langle H_\omega \rangle = \begin{pmatrix} 0 \\ v_2 \end{pmatrix}, \quad (5.23)$$

with

$$v_1 \equiv v \cos\beta \quad v_2 \equiv v \sin\beta, \quad (5.24)$$

where we have now reverted to the normalization where $v = 174$ GeV. When $v_1 \neq v_2$, then the estimate for $\delta\rho$ from the operators that break the custodial $SU(2)$ becomes,

$$\delta\rho = -v^2 [\cos^4\beta c_4^\chi + \sin^4\beta c_4^\omega - \cos^2\beta \sin^2\beta c_4^{\chi\omega}], \quad (5.25)$$

or

$$\delta\rho = \frac{N_c}{16\pi^2} \frac{g_{tc}^4 v^2}{4} \left[\frac{\cos^4\beta}{m_\chi^2} + \frac{\sin^4\beta}{m_\omega^2} - \frac{2\cos^2\beta \sin^2\beta}{m_\chi^2 - m_\omega^2} \ln \frac{m_\chi^2}{m_\omega^2} \right], \quad (5.26)$$

upon substituting in the matching contributions of equations (5.17) and (5.19). Even when the masses of the heavy fermions are equal, $m_\chi = m_\omega$, the perturbation to the ρ -parameter need not vanish:

$$\delta\rho = \frac{N_c}{16\pi^2} \frac{g_{tc}^4 v^2}{4} \frac{\cos^2 2\beta}{m_\chi^2}. \quad (5.27)$$

Returning to the $\tan\beta = 1$ case, we can obtain a larger bound on the mass of the ω by studying its effect on the ratio of decay widths $R_b \equiv \Gamma[Z \rightarrow b\bar{b}]/\Gamma[Z \rightarrow \text{hadrons}]$. The dominant contribution to R_b comes from the mixing of the ω and b fields. In passing from the weak eigenstates to the mass eigenstates, we perform a rotation

$$\begin{aligned} b_L &\rightarrow \cos\theta_L^\omega b_L - \sin\theta_L^\omega \omega_L \\ b_R &\rightarrow \cos\theta_R^\omega b_R - \sin\theta_R^\omega \omega_R, \end{aligned} \quad (5.28)$$

which shifts the $Zb\bar{b}$ couplings slightly. The standard model coupling of the Z to the left-handed b quark,

$$g_L^{b\text{sm}} = \left[\frac{1}{3} \sin^2\theta_W - \frac{1}{2} \right], \quad (5.29)$$

becomes after rotating the fields,

$$g_L^b = g_L^{b\text{sm}} \cos^2 \theta_L^\omega + g_L^\omega \sin^2 \theta_L^\omega \approx g_L^{b\text{sm}} + \frac{1}{2} \frac{m_{b\omega}^2}{m_\omega^2}, \quad (5.30)$$

to leading order. Here $m_{b\omega}$ is the dynamically generated mass that results from $b_L \omega_R$ condensation. Since b_R and ω_R have the same coupling to the Z , there is no shift in g_R . In the NJL approximation for a two doublet model, $m_{b\omega} = 400$ GeV. The mixing leads to a slight shift in the standard model prediction:

$$R_b = R_b^{\text{sm}} - 0.39 \frac{m_{b\omega}^2}{m_\omega^2}. \quad (5.31)$$

The standard model prediction, R_b^{sm} , is 0.2157 ± 0.0004 [22] while the most recent measurements yield $R_b = 0.21656 \pm 0.00074$ so that to agree to within 2σ requires

$$m_\omega > 25m_{b\omega} \sim 10 \text{ TeV}. \quad (5.32)$$

Apart from this tree-level mixing, the strongly coupled Higgs fields can also modify the width of $Z \rightarrow b\bar{b}$ through one-loop effects. We can estimate these effects using the effective theory given in equation (4.5),⁵

$$\mathcal{L}_{\text{eff}} = g_t \bar{\psi}_L^3 \mathcal{M} \lambda_R + \text{h.c.} \quad (5.33)$$

We shall show that most of the one-loop effects are generally small so we have neglected the Peccei-Quinn terms which are additionally suppressed by ξ . If we rotate these interactions into a mass eigenstate basis, as in equation (5.28) with an analogous pair of $t_{L,R} \rightarrow \chi_{L,R}$ rotations, we find the following couplings:

$$\begin{aligned} \bar{b}_L \mathcal{M}_1^2 \chi_R : g_t \cos \theta_L^\omega \cos \theta_R^\chi &\simeq \frac{m_{t\chi}}{v} \\ \bar{b}_L \mathcal{M}_1^2 t_R : g_t \cos \theta_L^\omega \sin \theta_R^\chi &\simeq \frac{m_t}{v} \\ \bar{b}_L \mathcal{M}_2^2 \omega_R : g_t \cos \theta_L^\omega \cos \theta_R^\omega &\simeq \frac{m_{b\chi}}{v} \\ \bar{b}_L \mathcal{M}_2^2 b_R : g_t \cos \theta_L^\omega \sin \theta_R^\omega &\simeq \frac{m_b}{v}, \end{aligned} \quad (5.34)$$

where the components of \mathcal{M} can be expanded about the $\tan \beta = 1$ vacuum according to equation (4.10). For $\tan \beta = 1$, using the Pagels-Stokar relation, we find $m_{b\omega} = m_{t\chi} \simeq 400$

⁵ Here we have assumed that the Higgs field has been renormalized so that we use the renormalized coupling constant $g_t = g_{tc}/\sqrt{Z_\phi}$, where Z_ϕ is given in equation (4.8).

GeV. Yukawa couplings involving $\bar{b}_R\chi_L$, $\bar{b}_R t_L$, and $\bar{b}_R\omega_L$ are all proportional to $\sin\theta_R^\omega \simeq m_b/v$ and are therefore negligible. From equation (5.34), we conclude that the dominant loop corrections are those shown in figures 9–11.

The diagrams of figure 9 have been studied previously [23] in the context of generic two-Higgs doublet models. The correction is negative and falls off as $1/m_{H^\pm}^2$ with increasing Higgs mass. A 300 GeV charged Higgs mass decreases R_b by about one σ . In any case for a lighter χ mass, a heavy charged Higgs is preferred and its effects will strengthen the bound (5.32) on the ω mass.

The diagrams of figures 10–11 involve the heavy isosinglet fermions χ and ω , both of which are strongly coupled to the composite Higgs scalars. We might therefore expect these corrections to be large. However, since the χ and ω are vectorlike, they can be given large $SU(2)_L$ -invariant masses and must decouple in the large mass limit. For this reason, the diagrams of figure 10 turn out to be quite small. For example, even with $m_{H^\pm} = 200$ GeV and $m_\chi = 1$ TeV, we find that these diagrams give

$$\delta R_b \simeq 2 \times 10^{-5},$$

which is indeed negligible. The neutral Higgs diagrams of figure 11 are negative and typically quite small. These corrections can be appreciable if there is a large mass splitting between the H^0 and the A^0 , in which case the diagrams grow as $\ln(m_{H^0}^2/m_{A^0}^2)$. For example, with $m_{A^0} = 100$ GeV, $m_{H^0} = 1$ TeV, $m_{h^0} = 200$ GeV, and $m_\omega = 2$ TeV, we find

$$\delta R_b \simeq -0.001.$$

The neutral Higgs effects can shift R_b by as much as one standard deviation in extreme cases. Finally, we note that the loop corrections scale as g_t^2 , which is inversely proportional to $\ln(M^2/m_\chi^2)$. We have taken this logarithm to be 5, corresponding to an order-of-magnitude difference between the topcolor scale and the masses of the χ and ω . The results should be scaled appropriately for models with different scales.

The corrections involving the Peccei-Quinn violating terms in the effective Lagrangian are expected to be smaller simply because the coupling in this case is weaker. For present purposes it is sufficient to retain only the Peccei-Quinn preserving part, with the caveat that the above results will likely be modified at the few percent level by the Peccei-Quinn breaking term.

In summary, despite the strong coupling between the weak-isosinglet fermions and the Higgs fields, we find that loop corrections involving these particles are typically small. The loop effects from the graphs in figure 9, however, do give a suppression of R_b when the Higgs mass is less than 500 GeV, which will strengthen the lower bound (5.32) on the mass of the ω .

The Higgs fields themselves contribute to S through⁶

$$S_{\text{higgs}} = \frac{1}{12\pi} \left[\ln \frac{m_{h^0}^2}{m_{h^0, \text{ref}}^2} + \frac{m_{H^0}^4 + m_{A^0}^4}{(m_{H^0}^2 - m_{A^0}^2)^2} + \frac{(m_{H^0}^2 - 3m_{A^0}^2)m_{H^0}^4}{(m_{H^0}^2 - m_{A^0}^2)^3} \ln \frac{m_{H^0}^2}{m_{H^\pm}^2} \right. \\ \left. - \frac{(m_{A^0}^2 - 3m_{H^0}^2)m_{A^0}^4}{(m_{H^0}^2 - m_{A^0}^2)^3} \ln \frac{m_{A^0}^2}{m_{H^\pm}^2} - \frac{11}{6} \right] \quad (5.35)$$

and to T through [24]

$$T_{\text{higgs}} = \frac{1}{32\pi \sin^2 \theta_W \cos^2 \theta_W M_Z^2} [f(m_{H^\pm}, m_{A^0}) + f(m_{H^\pm}, m_{H^0}) - f(m_{A^0}, m_{H^0})] \\ - \frac{3}{16\pi \cos^2 \theta_W} \ln \frac{m_{h^0}^2}{m_{h^0, \text{ref}}^2} \quad (5.36)$$

where the function $f(m_1, m_2)$ was defined in equation (5.3). We have used a reference value of $m_{h^0, \text{ref}} = 300 \text{ GeV}$ in our fits. Combining the Higgs and χ - ω contributions to S and T and comparing to the current experimental constraints on these parameters, we find the allowed values for m_χ and m_ω , for three illustrative Higgs masses, $m_{h^0} = 400, 800$ and 1200 GeV , shown in figure 12. When the Peccei-Quinn breaking terms are neglected, the masses of the heavy Higgs fields are degenerate, as seen in equation (4.11), so we have

⁶ The full contribution to S from the Higgs sector, with the standard model contributions subtracted out, is

$$\Delta S = \frac{1}{12\pi} \left[\cos^2(\beta - \alpha) \ln \frac{m_{H^0}^2}{m_{h^0}^2} - \frac{11}{6} \right. \\ + \sin^2(\beta - \alpha) \left(\frac{m_{H^0}^4 + m_{A^0}^4}{(m_{H^0}^2 - m_{A^0}^2)^2} + \frac{(m_{H^0}^2 - 3m_{A^0}^2)m_{H^0}^4 \ln \frac{m_{H^0}^2}{m_{H^\pm}^2} - (m_{A^0}^2 - 3m_{H^0}^2)m_{A^0}^4 \ln \frac{m_{A^0}^2}{m_{H^\pm}^2}}{(m_{H^0}^2 - m_{A^0}^2)^3} \right) \\ \left. + \cos^2(\beta - \alpha) \left(\frac{m_{h^0}^4 + m_{A^0}^4}{(m_{h^0}^2 - m_{A^0}^2)^2} + \frac{(m_{h^0}^2 - 3m_{A^0}^2)m_{h^0}^4 \ln \frac{m_{h^0}^2}{m_{H^\pm}^2} - (m_{A^0}^2 - 3m_{h^0}^2)m_{A^0}^4 \ln \frac{m_{A^0}^2}{m_{H^\pm}^2}}{(m_{h^0}^2 - m_{A^0}^2)^3} \right) \right]$$

where α and β are defined as in [15]. The case we are studying has $\beta = -\alpha = \pi/4$.

set $m_{h^0} = m_{H^0} = m_{H^\pm}$ in making these plots. We have also set $m_{A^0} = 100 \text{ GeV}$ to be safely above experimental limits.

As we mentioned above, for $m_{h^0} \approx 300 \text{ GeV}$, the corrections from the loops shown in figure 9 decrease R_b by one σ . In order to have R_b lie within the experimentally acceptable range then requires that the tree level corrections (5.31) be small which occurs when $m_\omega > 15 \text{ TeV}$. As we increase the common heavy Higgs mass, the loop corrections become less important and we can permit a larger tree level correction, which means that the bound on m_ω is relaxed to about 12 TeV for $m_{h^0} \approx 800 \text{ GeV}$. When the Higgs masses are of the order of 1 TeV or heavier, then the negative contribution to T from the Higgs fields must be compensated by a positive contribution from the heavy fermions, (5.22). This can only occur if the $m_\chi = m_\omega$ symmetry is badly broken. We see this effect appearing in figure 12 where the allowed values for m_χ are in the $3\text{--}5 \text{ TeV}$ range while $m_\omega > 15 \text{ TeV}$.

6. Conclusions.

We have presented a class of models that implement the top-condensate see-saw mechanism of electroweak symmetry breaking. The models accomplish all gauge symmetry breaking dynamically, without recourse to phenomenological Higgs scalars. The gauge structure of the models is complex. This complexity results mostly from the requirement that the models should admit higher dimensional gauge invariant operators that generate fermion masses and Yukawa couplings in the low energy theory. It may be possible to construct simpler models, once the flavor sector of the theory is better understood.

The models we have considered involve new isosinglet quarks. Models with only one such quark yield a low energy theory with one Higgs doublet, models with two yield two Higgs doublets. As with most models of dynamical symmetry breaking, the Higgs bosons are expected to be heavy. In the two doublet models, we expect a set of heavy ($\sim \text{TeV}$) charged and neutral scalars, together with a pseudoscalar which may be light ($\sim 100 \text{ GeV}$).

The new isosinglet quarks have measurable effects on low-energy physics. In one-doublet models, the heavy singlet χ can give a sizable contribution to the ρ parameter. This contribution constrains the mass of the χ to be between 5 and 8 TeV when the Higgs mass is above 500 GeV . In two doublet models, the contribution to ρ is small when the χ and ω are degenerate, since in this case the model has an $SU(2)_R$ custodial symmetry. The most stringent constraint on two-doublet models comes from $Z \rightarrow b\bar{b}$, which receives sizable

corrections from b - ω mixing. We have shown that the ω must at least be heavier than about 10 TeV. Loop corrections, while small for large Higgs masses and model dependent, make this bound much more stringent when the Higgs masses are less than about 500 GeV. The loop and tree level effects combine to impose a bound of $m_\omega > 12$ TeV.

A number of interesting issues have yet to be resolved. The models we have presented serve to illustrate the main issues involved in topcolor model-building. The gauge symmetries of these models are typically quite complex, and we might hope that a better understanding of the dynamics of these models, together with a better understanding of the flavor structure, will lead to simpler scenarios. We hope to return to these questions in later work.

References

- [1] The LEP Collaborations ALEPH, DELPHI, L3, OPAL, the LEP Electroweak Working Group and the SLD Heavy Flavour and Electroweak Groups, “A Combination of Preliminary Electroweak Measurements and Constraints on the Standard Model,” CERN-EP/99-15.
- [2] M. S. Chanowitz, “Combining real and virtual Higgs boson mass constraints,” Phys. Rev. Lett. **80** (1998) 2521; [hep-ph/9710308](#). R. S. Chivukula and N. Evans, “Triviality and the precision bound on the Higgs mass,” [hep-ph/9907414](#).
- [3] M. E. Peskin and T. Takeuchi, “Estimation of oblique electroweak corrections,” Phys. Rev. **D46** (1992) 381.
- [4] For a review, see E. Farhi and L. Susskind, “Technicolor,” Phys. Rept. **74** (1981) 277.
- [5] W. A. Bardeen, C. T. Hill and M. Lindner, “Minimal dynamical symmetry breaking of the standard model,” Phys. Rev. **D41** (1990) 1647
- [6] Bogdan A. Dobrescu and Christopher T. Hill, “Electroweak Symmetry Breaking via a Top Condensation Seesaw Mechanism,” Phys. Rev. Lett. **81** (1998) 2634; [hep-ph/9712319](#).
- [7] C. T. Hill, “Topcolor: Top quark condensation in a gauge extension of the standard model,” Phys. Lett. **B266**, (1991) 419; C. T. Hill, “Topcolor assisted technicolor,” Phys. Lett. **B345** (1995) 483, [hep-ph/9411426](#).
- [8] Y. Nambu, report EFI 88-39 (July 1988), published in the Proceedings of the *Kazimierz 1988 Conference on New theories in physics*, ed. T. Eguchi and K. Nishijima; in the Proceedings of the *1988 International Workshop on New Trends in Strong Coupling Gauge Theories*, Nagoya, Japan, ed. Bando, Muta and Yamawaki (World Scientific, 1989); report EFI-89-08 (1989); V. A. Miransky, M. Tanabashi and K. Yamawaki, Mod. Phys. Lett. **A4** (1989) 1043; Phys. Lett. **B 221** (1989) 177; W. J. Marciano, Phys. Rev. Lett. **62** (1989) 2793.
- [9] H. Pagels and S. Stokar, “The Pion Decay Constant, Electromagnetic Form-Factor And Quark Electromagnetic Selfenergy In QCD,” Phys. Rev. **D20** (1979) 2947.
- [10] R. Sekhar Chivukula, Bogdan A. Dobrescu, Howard Georgi, Christopher T. Hill, “Top Quark Seesaw Theory of Electroweak Symmetry Breaking,” Phys. Rev. **D59** (1999) 075003; [hep-ph/9809470](#).
- [11] H. Georgi, “Generalized Dimensional Analysis,” Phys. Lett. **B298** (1993) 187; [hep-ph/9207278](#).
- [12] H. Georgi, “A Tool Kit For Builders Of Composite Models,” Nucl. Phys. **B266** (1986) 274; H. Georgi, “ $SU(2) \times U(1)$ breaking, compositeness and flavor,” Les Houches, 1985 (North-Holland, 1987) 339.
- [13] H. Georgi, A. Grant and H. Collins, [hep-ph/9907477](#).

- [14] Y. Nambu and G. Jona-Lasinio, “Dynamical Model Of Elementary Particles Based On An Analogy With Superconductivity. I,” *Phys. Rev.* **122** (1961) 345.
- [15] J. F. Gunion, H. E. Haber, G. Kane, and S. Dawson, *The Higgs Hunter’s Guide*, Addison-Wesley Publishing Company, 1990.
- [16] Particle Data Group, “Review of Particle Physics,” *Eur. Phys. J.* **C3** (1998) 1.
- [17] B. Grinstein and M. Wise, “Operator analysis for precision electroweak physics,” *Phys. Lett.* **B265** (1991) 326.
- [18] D. Toussaint, “Renormalization Effects from Superheavy Higgs Particles,” *Phys. Rev.* **D18** (1978) 1626.
- [19] M. Golden and L. Randall, “Radiative Corrections to Electroweak Parameters in Technicolor Theories,” *Nucl. Phys.* **B361** (1991) 3–23.
- [20] D. Bardin *et al.*, “ZFITTER: An Analytical program for fermion pair production in e^+e^- annihilation,” CERN-TH. 6443/92; [hep-ph/9412201](#).
- [21] See for example the references cited in the table H^0 **Indirect Mass Limits from Electroweak Analysis** on page 247 of Particle Data Group, “Review of Particle Physics,” *Eur. Phys. J.* **C3** (1998) 1.
- [22] C. T. Hill and X. Zhang, “ $Z \rightarrow b\bar{b}$ versus Dynamical Electroweak Symmetry Breaking Involving the Top Quark,” *Phys. Rev.* **D51** (1995) 3563.
- [23] A. Denner, R. J. Guth, W. Hollik, and J. H. Kuhn, “The Z width in the two Higgs doublet model,” *Z. Phys.* **C51** (1991) 695. A. K. Grant, “Implications of a heavy top quark for the two Higgs doublet model,” *Phys. Rev.* **D51** (1995) 207; [hep-ph/9410267](#).
- [24] A. Denner, R. J. Guth and J. H. Kuhn, “Relaxation Of Top Mass Limits In The Two Higgs Doublet Model,” *Phys. Lett.* **B240** (1990) 438.

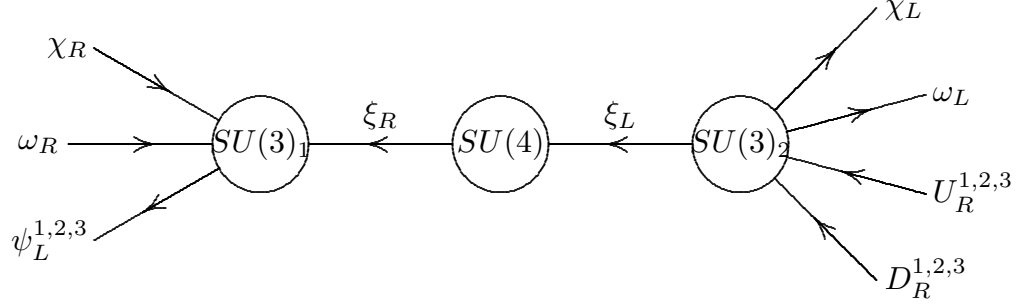


Figure 1. An example of a simple model that can realize a topcolor seesaw. The central gauge group is chosen so that the theory is free of anomalies.

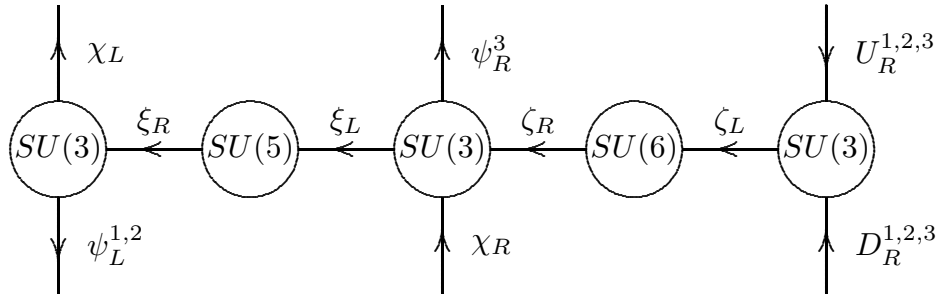


Figure 2. Another topcolor theory constructed so that $\bar{\chi}_L t_R$ and $\bar{\chi}_R \chi_L$ terms are forbidden at tree-level. Instead, these terms arise dynamically in the low energy theory.

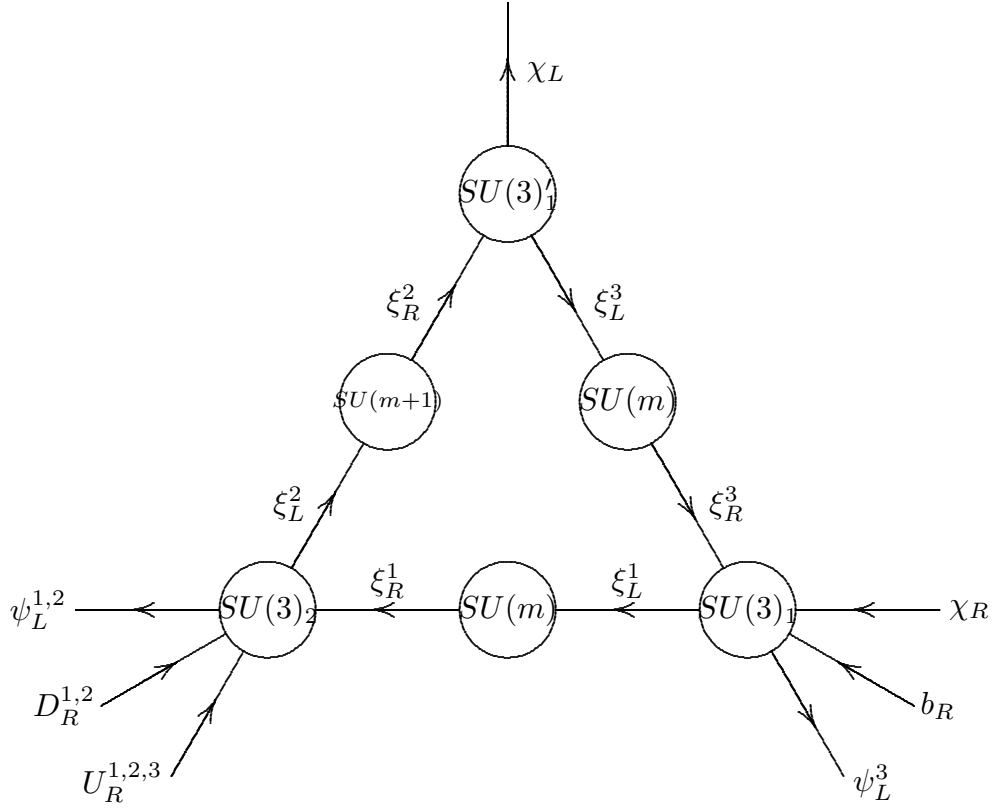


Figure 3. Chivukula, Dobrescu, Georgi, and Hill's topcolor model [10]. The low energy

effective theory for this model contains a single composite Higgs double.

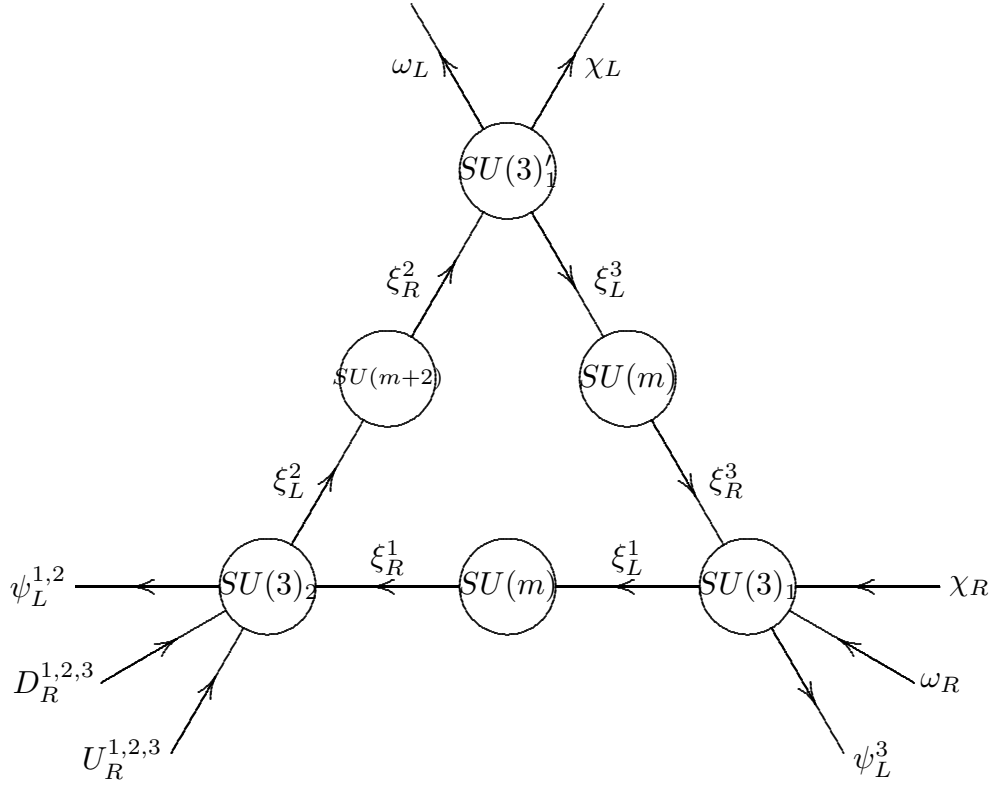


Figure 4. Another topcolor model which contains two composite Higgs doublets in the low energy effective theory.

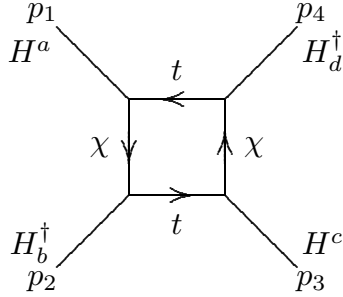


Figure 5. This diagram gives the leading matching contribution to the operator that violates custodial $SU(2)$ in the effective theory for energies below the χ mass.

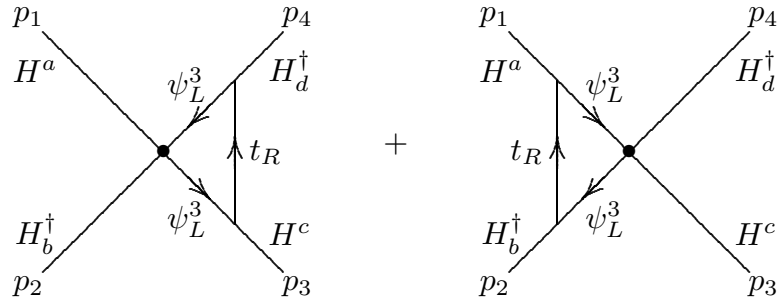


Figure 6. These graphs gives the leading running contribution to the operator in the low energy theory that violates custodial $SU(2)$.

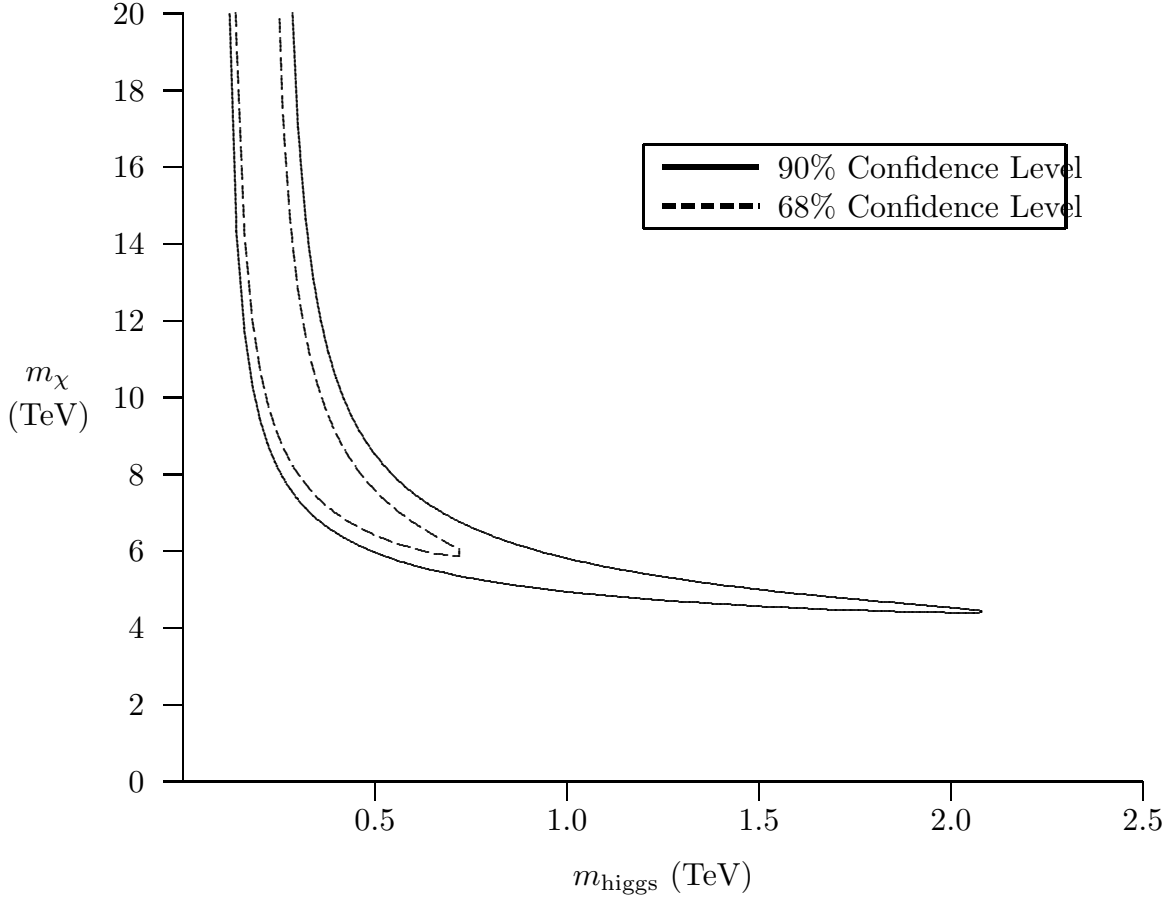


Figure 7. The allowed set of m_χ and m_{higgs} masses based on current precision electroweak tests.

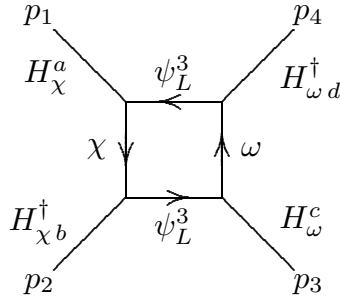


Figure 8. This graph produces the leading matching contribution to the custodial $SU(2)$ -violating operator $\mathcal{O}_4^{\chi\omega}$.

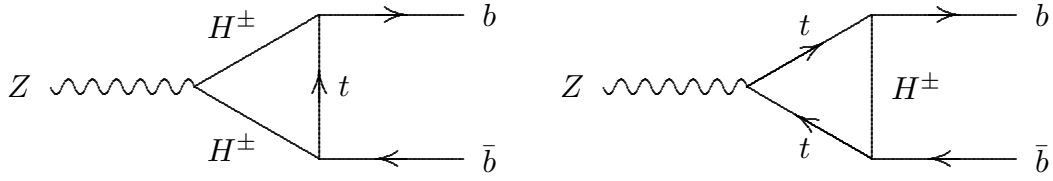


Figure 9. These diagrams produce the dominant one-loop corrections which involve only the third generation fermions and the appropriate Higgs fields.

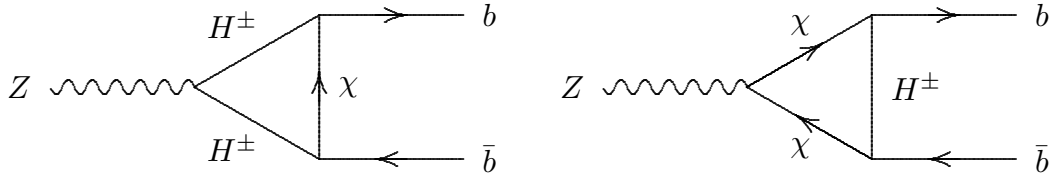


Figure 10. These diagrams produce the dominant one-loop corrections which involve the χ fermion.

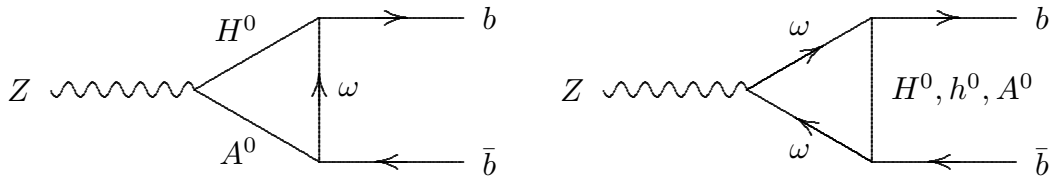


Figure 11. These diagrams produce the dominant one-loop corrections which involve the ω fermion.

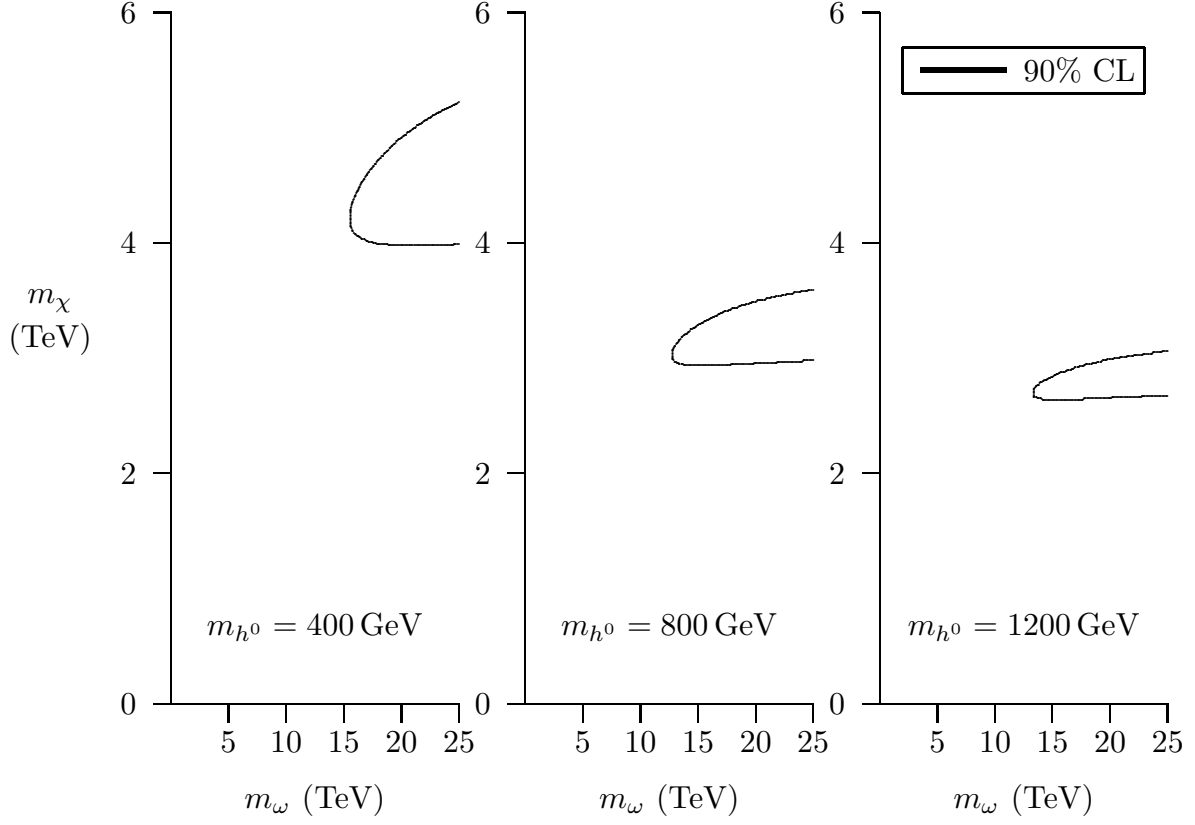


Figure 12. This figure shows the regions in the χ - ω mass plane allowed by the current precision electroweak experiments when the massive Higgs fields, h^0 , H^0 and H^\pm , have a common mass of 400, 800 and 1200 GeV respectively. In each of these plots, the light pseudoscalar Higgs field, A^0 , was given a mass of 100 GeV.